

Supporting Information

Polyoxometalate-assisted Formation of CoSe/MoSe₂ Heterostructures with Enhanced Oxygen Evolution Activity

Menglei Yuan, Sobia Dipazir, Meng Wang, Yu Sun, Denglei Gao, Yiling Bai, Min Zhang, Peilong Lu, Hongyan He, Xiangyang Zhu, Jingxian Zhang, Shuwei Li, Zhanjun Liu, Zhaopeng Luo and Guangjin Zhang*

Fig. S1 SEM images of (a) PMo₁₂@ZIF-67 and (b) ZIF-67.

Fig. S2 XRD patterns of CoSe/MoSe₂-700, CoSe/MoSe₂-800 and CoSe/MoSe₂-900.

Fig. S3 SEM images of (a) CoSe and (b) MoSe₂.

Fig. S4 H₂-TPR profiles for CoSe/MoSe₂-700, CoSe/MoSe₂-800 and CoSe/MoSe₂-900.

Fig. S5 Fermi level (E_F), valence band maximum (E_V) and onset level (Eonset) of UPS spectra for CoSe/MoSe₂-900.

Fig. S6 NH₃-TPD profiles for CoSe and CoSe/MoSe₂-900.

Fig. S7 N₂ adsorption/desorption isotherm of (a) CoSe, (c) MoSe₂, (e) CoSe/MoSe₂-700, (g) CoSe/MoSe₂-800, (i) CoSe/MoSe₂-900 and the corresponding pore size distribution of (b) CoSe, (d) MoSe₂, (f) CoSe/MoSe₂-700, (h) CoSe/MoSe₂-800, (j) CoSe/MoSe₂-900.

Fig. S8 (a) Nyquist plots of electrochemical impedance spectra (EIS) of CoSe/MoSe₂-700, CoSe/MoSe₂-800 and CoSe/MoSe₂-900; (b) XPS spectra of N 1s for CoSe/MoSe₂-700, CoSe/MoSe₂-800 and CoSe/MoSe₂-900.

Fig. S9 CV curves of (a) CoSe/MoSe₂-900; (b) CoSe/MoSe₂-800; (c) CoSe/MoSe₂-700; (d) CoSe; (e) MoSe₂ with different rates from 20 to 140 mV/s; (f) ΔJ of catalysts plotted against scan rate at the potential of 1.25 V vs. RHE. The slopes were used to denote the ECSA.

Fig. S10 SEM images of (a), (c) of CoSe/MoSe₂-900-50 and (b), (d) CoSe/MoSe₂-900-75; (e) The

OER polarization curves of CoSe/MoSe₂-900-50 and CoSe/MoSe₂-900-75 and (f) the corresponding Tafel plots.

Fig. S11 The estimated Faradic efficiency of CoSe/MoSe₂-900 as function of the current density.

Fig. S12 Time-dependent current density curve of of CoSe/MoSe₂-900 under a static overpotential of 343 mV for 36000s.

Fig. S13 Polarization curves of CoSe/MoSe₂-900 in 30 wt% KOH.

Fig. S14 (a) The structure model of CoSe (002)/MoSe₂(103); (b) Planar-averaged electron density difference $\Delta P(z)$ of CoSe (002)/MoSe₂(103). Inset is the 3D isosurface of the electron density difference , where the yellow and cyan areas represent electron accumulation and depletion, respectively, and the isosurface value is set to be 0.0004 e/ \AA^3 .

Fig. S15 SEM images of CoSe/MoSe₂-900 (a) before and (b) after OER testing.

Table S1 Comparison of OER activity of CoSe/MoSe₂-900 with previously reported MOF-derived materials in 1.0 M KOH solution.

Table S2 Comparison of OER activity of CoSe/MoSe₂-900 with previously reported Co-based materials in 1.0 M KOH solution.

Table S3 The ICP-OES measurements of CoSe, MoSe₂, CoSe/MoSe₂-700, CoSe/MoSe₂-800, CoSe/MoSe₂-900.

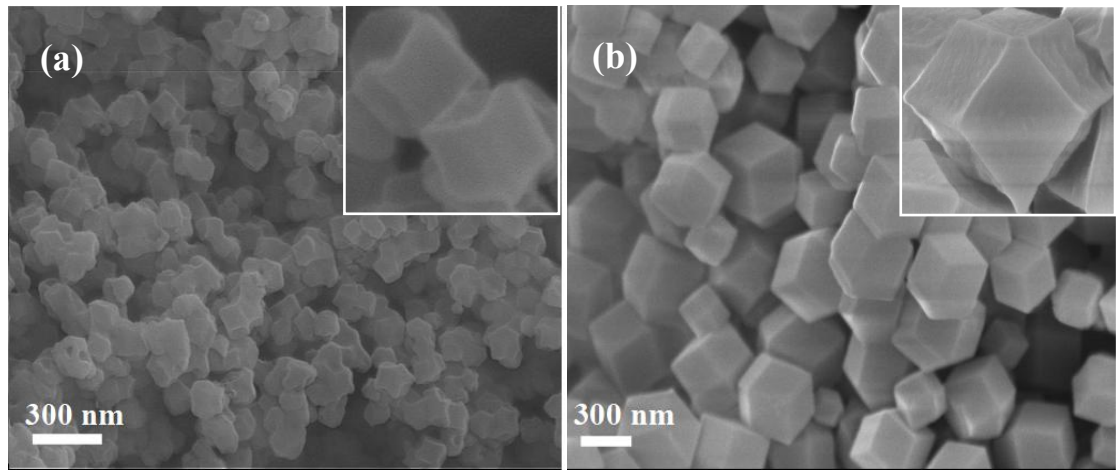


Fig. S1 SEM images of (a) PMo₁₂@ZIF-67 and (b) ZIF-67.

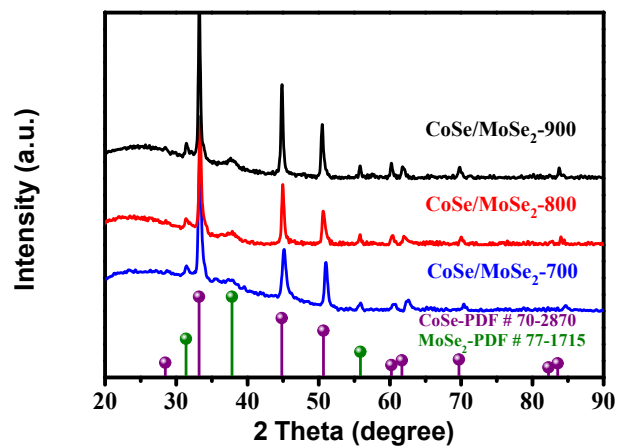


Fig. S2 XRD patterns of CoSe/MoSe₂-700, CoSe/MoSe₂-800 and CoSe/MoSe₂-900.

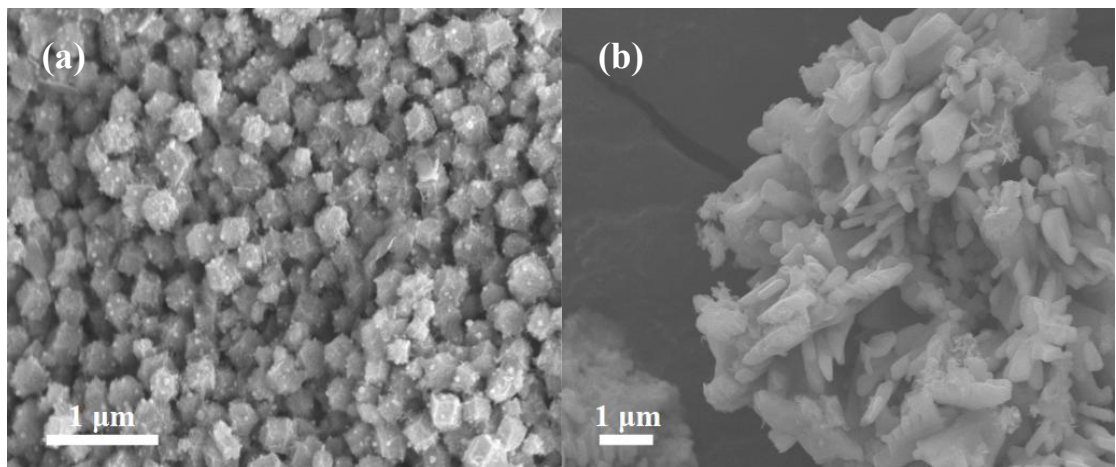


Fig. S3 SEM images of (a) CoSe and (b) MoSe₂.

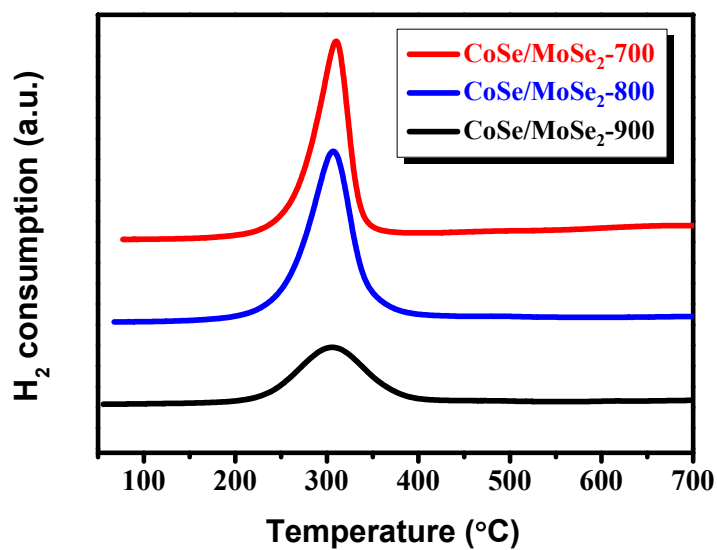


Fig. S4 H₂-TPR profiles for CoSe/MoSe₂-700, CoSe/MoSe₂-800 and CoSe/MoSe₂-900.

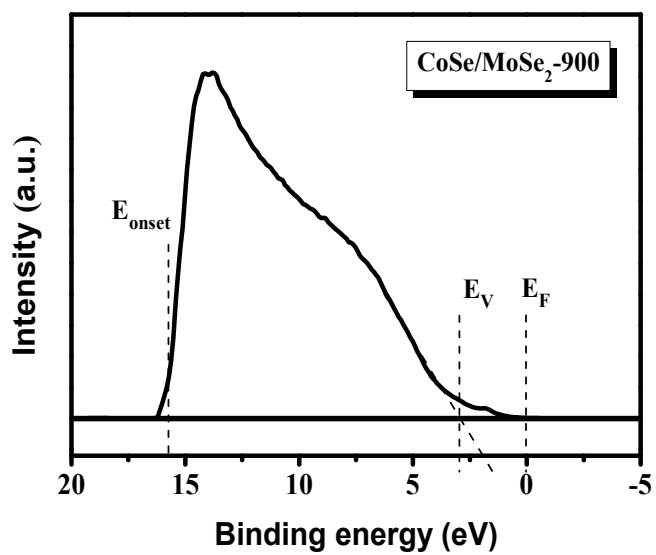


Fig. S5 Fermi level (E_F), valence band maximum (E_V) and onset level (E_{onset}) of UPS spectra for CoSe/MoSe₂-900.

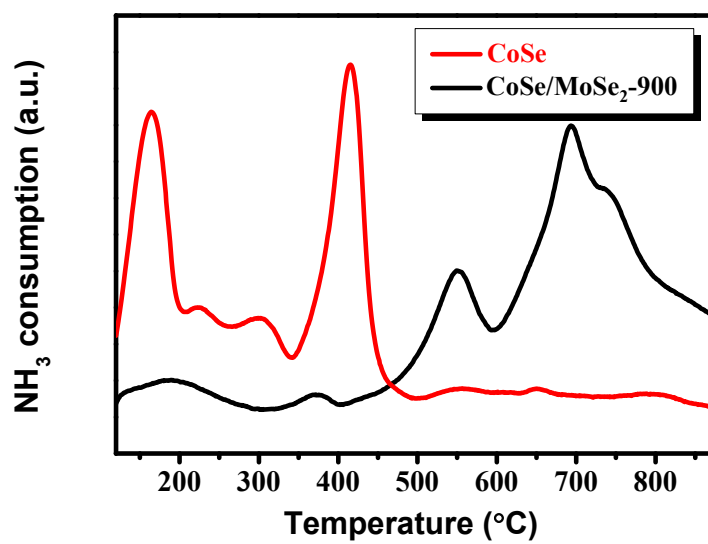


Fig. S6 NH₃-TPD profiles for CoSe and CoSe/MoSe₂-900.

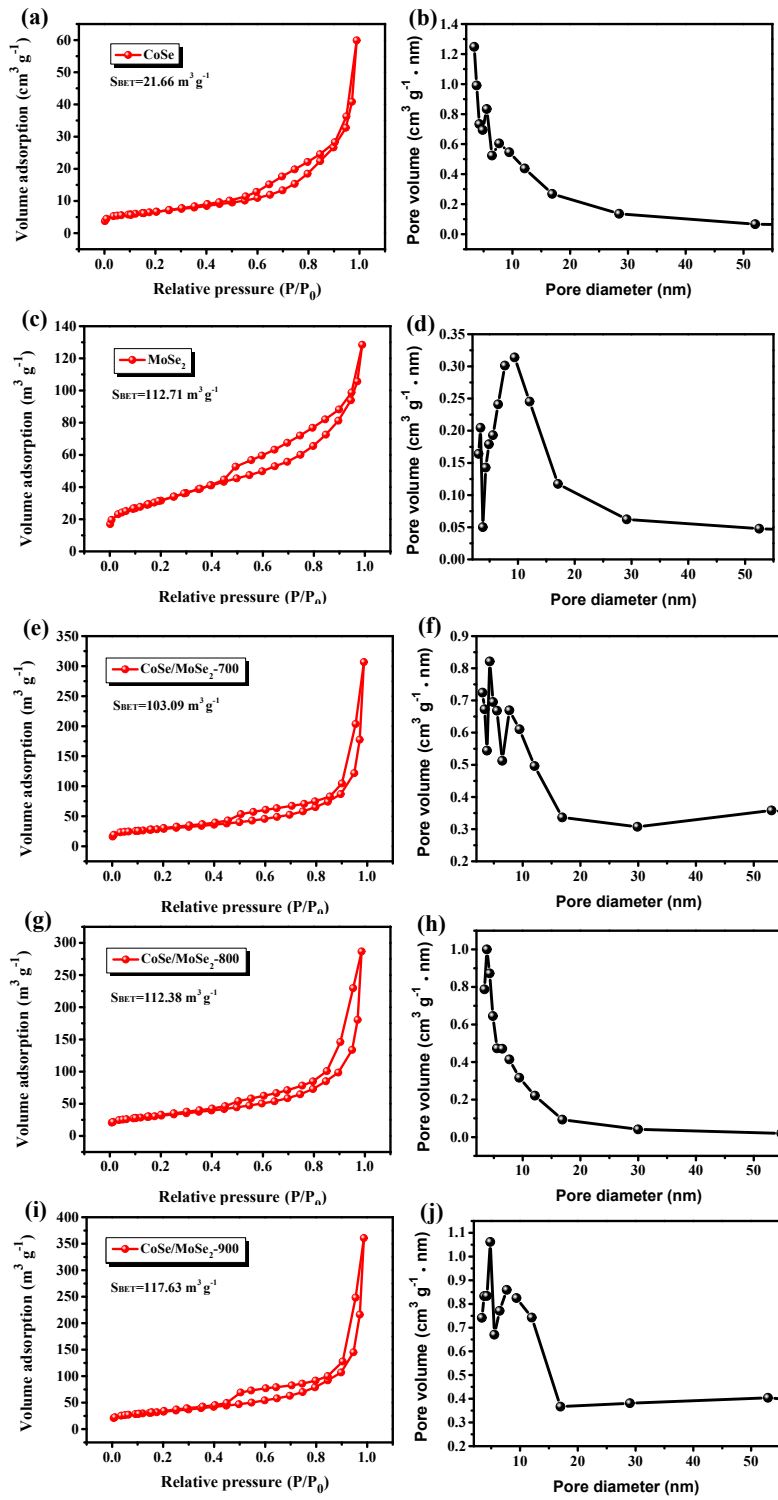


Fig. S7 N₂ adsorption/desorption isotherm of (a) CoSe, (c) MoSe₂, (e) CoSe/MoSe₂-700, (g) CoSe/MoSe₂-800, (i) CoSe/MoSe₂-900 and the corresponding pore size distribution of (b) CoSe, (d) MoSe₂, (f) CoSe/MoSe₂-700, (h) CoSe/MoSe₂-800, (j) CoSe/MoSe₂-900.

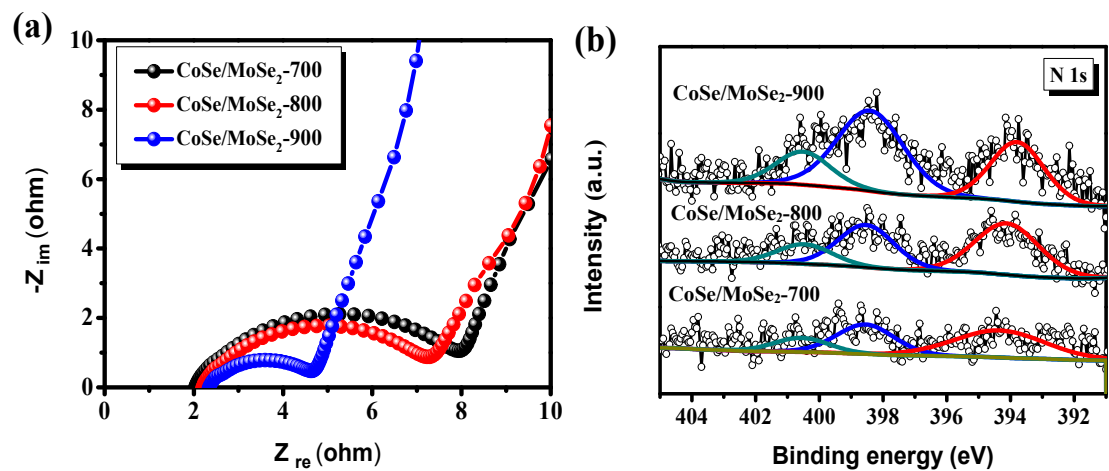


Fig. S8 (a) Nyquist plots of electrochemical impedance spectra (EIS) of CoSe/MoSe₂-700, CoSe/MoSe₂-800 and CoSe/MoSe₂-900; (b) XPS spectra of N 1s for CoSe/MoSe₂-700, CoSe/MoSe₂-800 and CoSe/MoSe₂-900.

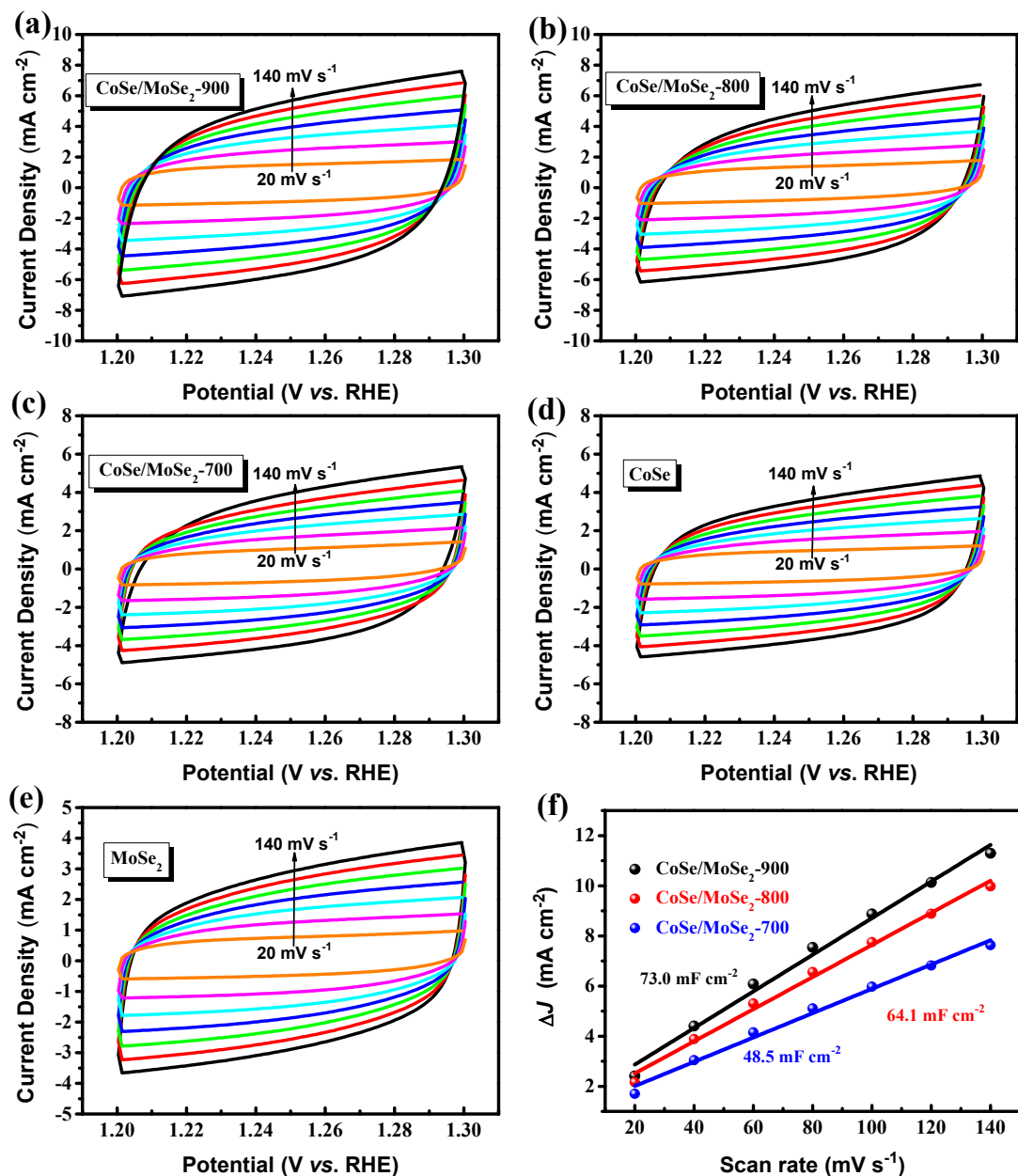


Fig. S9 CV curves of (a) CoSe/MoSe₂-900; (b) CoSe/MoSe₂-800; (c) CoSe/MoSe₂-700; (d) CoSe; (e) MoSe₂ with different scan rates from 20 to 140 mV/s ; (f) ΔJ of catalysts plotted against scan rate at the potential of 1.25 V vs. RHE. The slopes were used to denote ECSA.

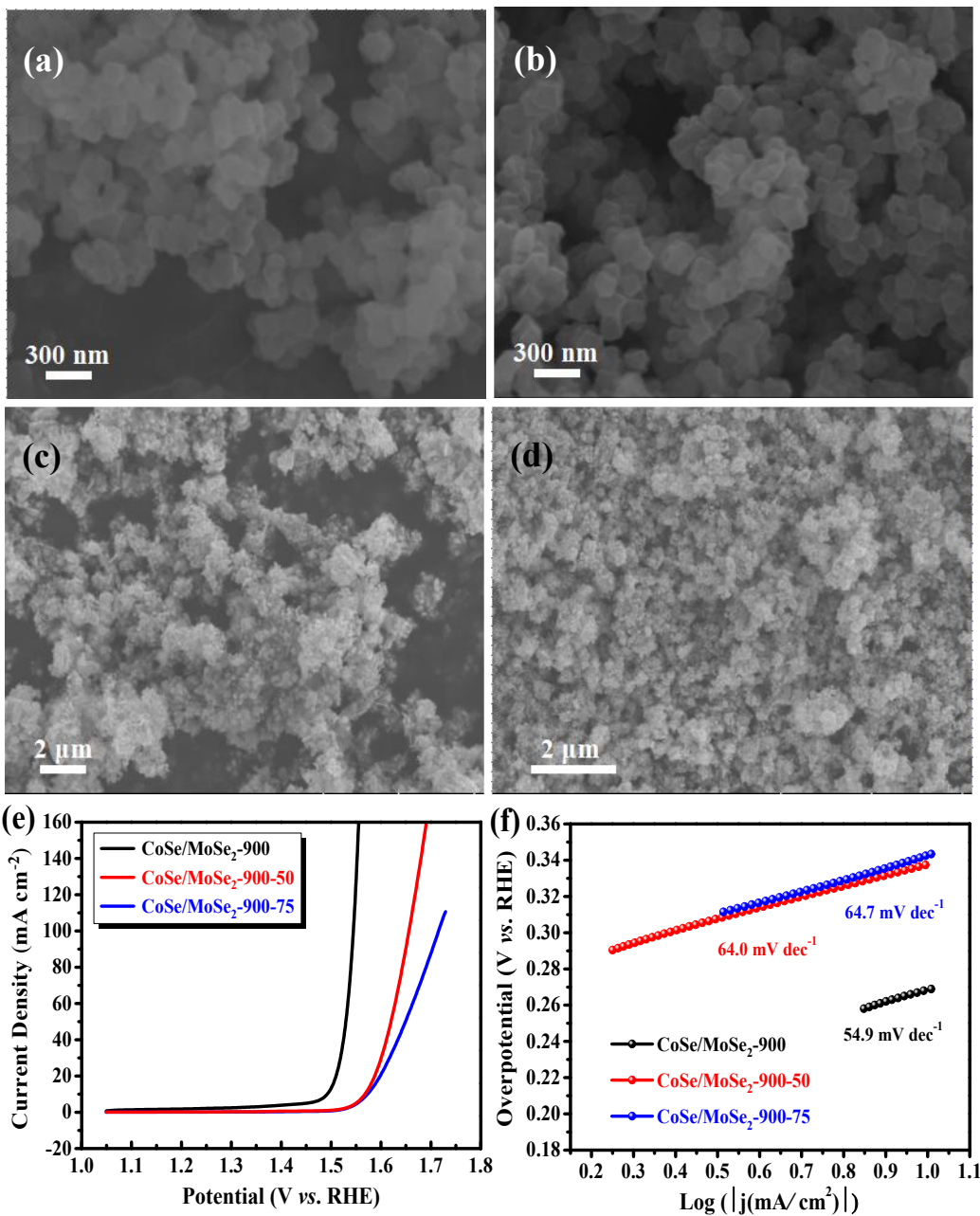


Fig. S10 SEM images of (a), (c) of CoSe/MoSe₂-900-50 and (b), (d) CoSe/MoSe₂-900-75; (e) The OER polarization curves of CoSe/MoSe₂-900-50 and CoSe/MoSe₂-900-75 and (f) the corresponding Tafel plots.

Note: we changed the mass of PMo₁₂ to 50 mg and 75 mg during the preparation of the PMo₁₂@ZIF-67 precursors. The subsequent preparation process was the same as CoSe/MoSe₂-900 to obtain CoSe/MoSe₂-900-50 and CoSe/MoSe₂-900-75 catalysts.

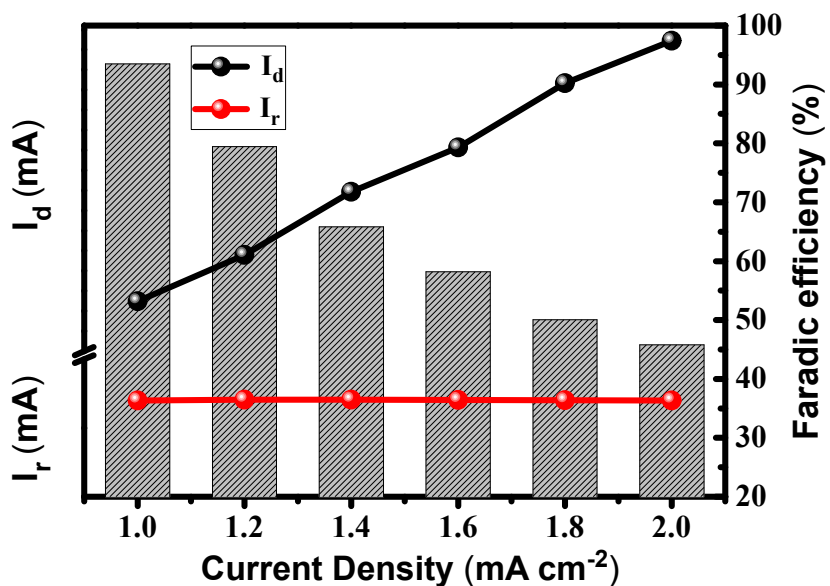


Fig. S11 The estimated Faradic efficiency of CoSe/MoSe₂-900 as function of the current density.

Rotating ring-disk electrode (RRDE) equipment was used to test the Faradaic efficiency of CoSe/MoSe₂-900 the catalysts during the OER process. As for the RRDE measurements, series of current density steps from 1 to 2 mA cm^{-2} were applied to the ring electrode at 0.2 V (vs.RHE). And the corresponding ring current was also collected to check the Faradaic efficiency change with the catalytic process. The Faradaic efficiency was calculated according to:

$$\text{Faradic efficiency} = (2 * I_r) / (n * I_d)$$

Where I_r and I_d are ring and disk current respectively; N is collection efficiency of ring electrode.

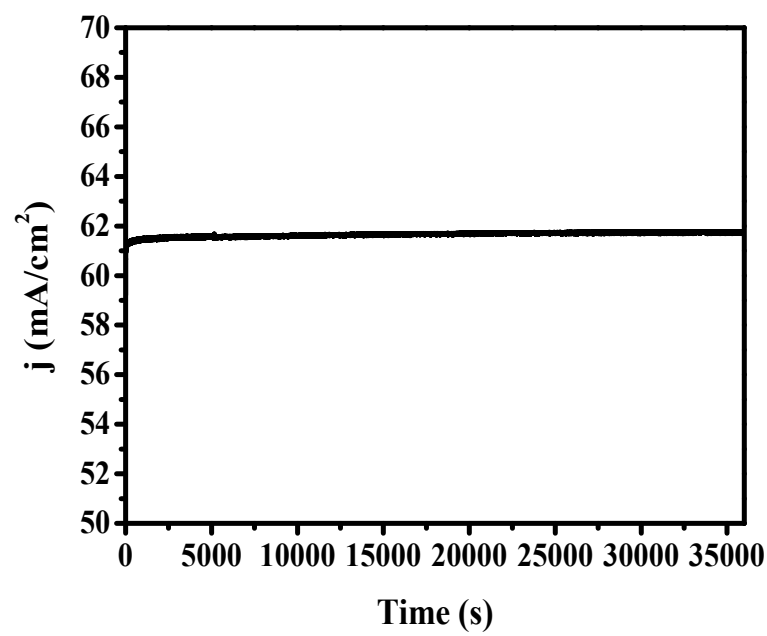


Fig. S12 Time-dependent current density curve of CoSe/MoSe₂-900 under a static overpotential of 343 mV for 36000s.

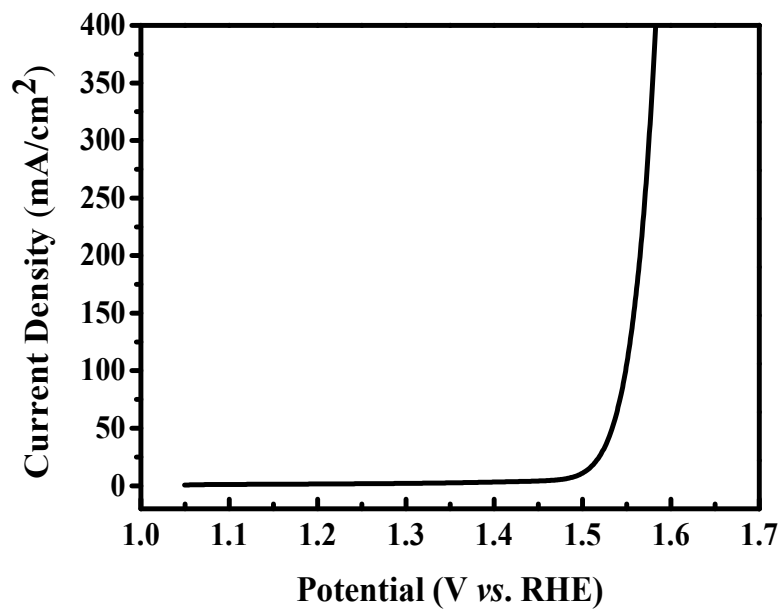


Fig. S13 Polarization curves of CoSe/MoSe₂-900 in 30 wt% KOH.

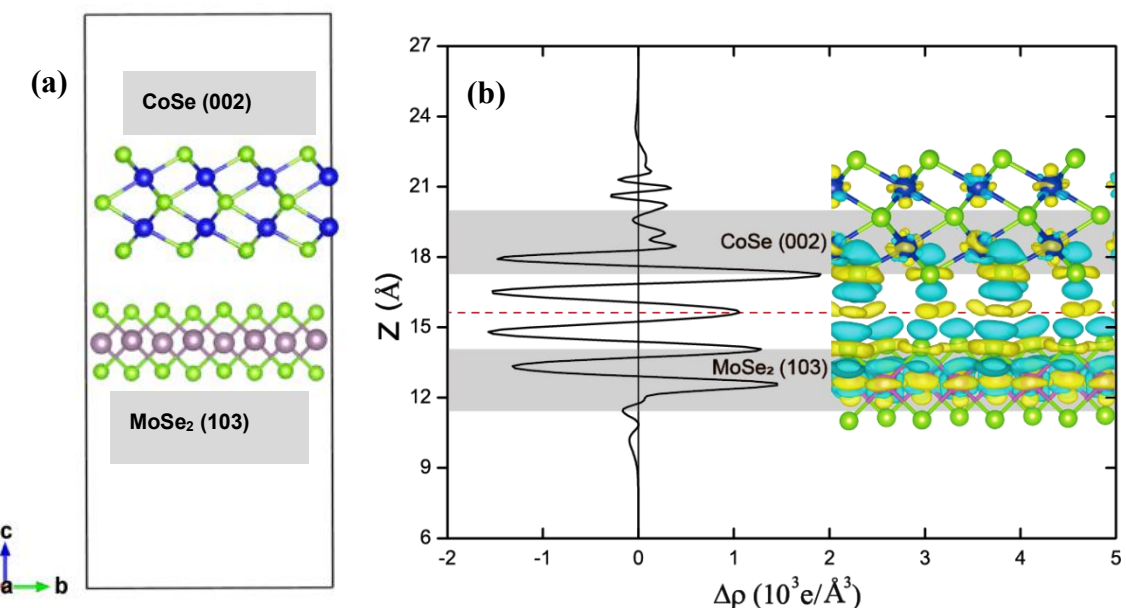


Fig. S14 (a) The structure model of CoSe (002)/MoSe₂(103); (b) Planar-averaged electron density difference ΔP (z) of CoSe (002)/MoSe₂(103). Inset is the 3D isosurface of the electron density difference , where the yellow and cyan areas represent electron accumulation and depletion, respectively, and the isosurface value is set to be $0.0004 \text{ e}/\text{\AA}^3$.

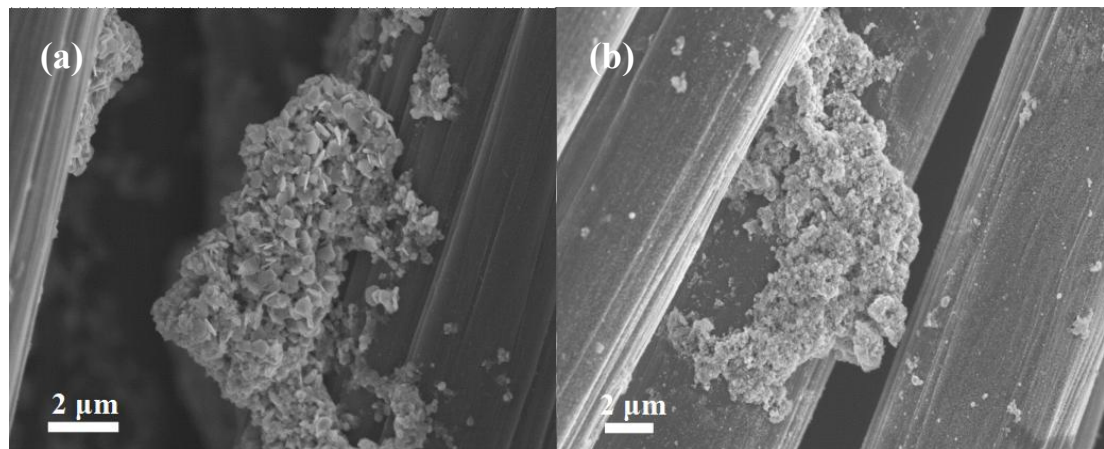


Fig. S15 SEM images of CoSe/MoSe₂-900 (a) before and (b) after OER testing.

Table S1 Comparison of OER activity of CoSe/MoSe₂-900 with previously reported MOF-derived materials in 1.0 M KOH solution.

Catalysts	Mass loading (mg/cm ²)	Electrolyte	Overpotential at 10 mA cm ⁻² (mV vs. RHE)	Tafel slope (mV/d ec)	Reference
CoSe/MoSe ₂ -900	0.3	1 M KOH	262	54.9	This work
CeOx/CoS	0.2	1 M KOH	269	50	Angew.Chem.Int.Ed.,2018,57,8654
NiCo@NiCoO ₂ core@shell nanoparticles	3.2	1 M KOH	~335	83.97	Adv. Mater.,2018,21,1705442
Ni-MOF@Fe-MOF	0.2	1 M KOH	265	82	Adv. Funct. Mater.,2018,28,1801554
Co ₃ O ₄ /CoMoO ₄ -50	0.255	1 M KOH	318	63	J.Mater.Chem.A.,2018,6, 1639-1647
CoNi(20:1)-P-NS	0.153	1 M KOH	273	45	Energy Environ Sci,2017,10,893
(Ni _{0.62} Fe _{0.38}) ₂ P	0.3	1 M KOH	290	44	Catal. Sci. Technol,2017,7,1549
Ni@NC-800	0.31	1M KOH	280	45	Adv. Mater,2017,29,1605957
A-CoS _{4.6} O _{0.6}	0.8	1 M	290	67	Angew.Chem.Int.Ed.,2017,56,4858

PNCs		KOH			
Ni-Co mixed oxide cages	-	1 M KOH	380	50	Adv. Mater,2016,18,4601
Zn-doped CoSe ₂ /CFC	-	1 M KOH	356	88	ACS Appl.Mater.Interfaces.,2016,8,2690 2-26907
Co ₃ O ₄ /NiCo ₂ O ₄ cages	1	1 M KOH	340	88	J.Am.Chem.Soc.,2015,137, 5590

Table S2 Comparison of OER activity of CoSe/MoSe₂-900 with previously reported Co-based materials in 1.0 M KOH solution.

Catalysts	Mass loading (mg/cm ²)	Electrolyte	Overpotential at 10 mA cm ⁻² (mV vs. RHE)	Tafel slope (mV/d ec)	Reference
CoSe/MoSe ₂ -900	0.3	1 M KOH	262	54.9	This work
CeOx/CoS	0.2	1 M KOH	269	50	Angew.Chem.Int.Ed.,2018,57,8654
NiCo@NiCoO ₂ core@shell nanoparticles	3.2	1 M KOH	~335	83.97	Adv. Mater.,2018,21,1705442
Co ₃ O ₄ /CoMoO ₄ -50	0.255	1 M KOH	318	63	J.Mater.Chem.A.,2018,6, 1639-1647
CoxMoy@NC	-	1 M KOH	330	46	J.Mater.Chem.A.,2017,5, 16929
NiCo LDHs	-	1 M KOH	367	40	Nano. Lett,2015,15,1421
Co ₃ S ₄ @MoS ₂	0.283	1M KOH	330	59	Chem. Mater,2017,29,5566
Fe-CoOOH	0.20	1 M KOH	330	37	Adv. Energy. Mater,2017,7,1602148

Co₃O₄/Fe₂O₃ nanocubes	3.0	1 M KOH	310	67	Chem. Eng. J, 2019, 355, 336
Ni_{2.5}Co_{0.5}Fe/N F	0.25	1 M KOH	275	99	J.Mater.Chem.A., 2016, 4, 7245
NixCo_{2x}(OH)₆ x@Ni	-	1 M KOH	305	78	J. Power.Sources., 2016, 317, 1

Table S3 The ICP-OES measurements of CoSe, MoSe₂, CoSe/MoSe₂-700, CoSe/MoSe₂-800, CoSe/MoSe₂-900.

	<i>CoSe</i>	<i>MoSe₂</i>	<i>CoSe/MoSe₂-700</i>	<i>CoSe/MoSe₂-800</i>	<i>CoSe/MoSe₂-900</i>
<i>Co(%)</i>	11.21	-----	10.92	10.34	11.04
<i>Mo(%)</i>	-----	1.26	1.104	1.152	1.485